

PHYSICAL AND MATHEMATICAL MODELLING OF CRACK-TIP  
BLUNTING IN C-Mn FERRITIC-PEARLITIC STEELS

R. Roberti\* and D. Firrao\*\*

Experiments have been performed on a C-Mn ferritic-pearlitic steel with an overall composition almost identical to a few previously tested steels of the same class. The steel had an inclusion spacing considerably larger than before. Results of fracture toughness tests on varying notch root radius specimens have once again demonstrated the similarity between the radius of curvature reached by the crack-tip upon blunting and the mean distance between larger sulfides embedded in the matrix. Furthermore, a  $J_{IC}$  increase similar to the interparticle spacing augment has been obtained. Fracture toughness and inclusion content data have been used to further validate a physical and mathematical model previously proposed by the authors to interpret ductile fracture toughness data in mild steels.

INTRODUCTION

A model describing the phenomena intervening during the process of ductile fracture nucleation and extension from a pre-existing crack in mild steel components has been recently proposed by the authors (1). It encompasses several stages under increasing applied stresses; (i) initial crack-tip blunting and void nucleation around first-row large second-phase particles, (ii) increase of the radius of curvature of the blunted tip up to a limiting value and cocurrent joining of the crack-front to first-row enlarged voids, (iii) further straining of the remaining ligaments between enveloped voids up to their rupture that marks the final overall crack advance.

It follows that the level of fracture toughness ( $J_{IC}$ ) in mild steels is in effect determined by the amount of plastic yielding intervening in stages (ii) and (iii) at the stress concentration prior to the ligament failure; next, the extension of such a deformation process is in turns governed by the micro-

\*Dipartimento di Chimica-Fisica Applicata, Politecnico di Milano, Italy.

\*\*Dipartimento di Scienza dei Materiali e Ingegneria Chimica, Politecnico di Torino, Italy.

structural features of the steel. In fact, as regards stage (ii), the limiting value of the radius of curvature achieved by the crack-tip during blunting is almost identical to the spacing among major inclusions, as already demonstrated by Knott et al (2, 3) and by Firrao and Roberti (4). The resistance to the real crack advance (stage iii) is then determined by the capacity of the matrix material between pores to continue to flow up to a limiting fracture strain. The level of such a property is enhanced by the ability of the matrix to strain-harden and is foreshortened by its tendency to strain localization; it therefore depends on the total inclusion volume fraction and the local state of stress (Hahn and Rosenfield (5)).

The above described physical model has led the authors (4) to the following mathematical formulation for ductile fracture toughness,

$$J_{IC} = \sigma_y^{(1-N)} \cdot \epsilon_{max,f}^{*(1+N)} \cdot E^N \cdot \underline{s} / F(\Gamma(N)) \dots\dots\dots(1)$$

Eq. 1 has been derived from the mathematical relationship proposed by Rice (6) among the J-integral applied to a blunt notch specimen, the notch-end radius,  $\rho$ , the strain hardening properties of a material, and the maximum strain acting at the notch root,  $\epsilon_{max}$ ,

$$\epsilon_{max}^* = \epsilon_y \cdot \{ [F(\Gamma(N)) \cdot J] / [\sigma_y \cdot \epsilon_y \cdot \rho] \}^{1/(1+N)} \dots\dots\dots(2)$$

If the maximum strain acting at the notch root at fracture initiation is always the same whichever the value of  $\rho$ , the above equation becomes a criterion for fracture and can be written,

$$\epsilon_{max,f}^* = \epsilon_y \cdot \{ [F(\Gamma(N)) \cdot J_C] / [\sigma_y \cdot \epsilon_y \cdot \rho] \}^{1/(1+N)} \dots\dots\dots(3)$$

For a given material, Eq. 3 depicts a straight line passing through the origin of the  $J_C$ - $\rho$  field, with its angular coefficient being a function of  $\epsilon_{max,f}^*$ . For  $\rho$ 's smaller than a limiting value the above equation loses its physical meaning. Such a limiting value, usually referred to as  $\rho_{eff}$ , is the maximum notch-end radius that causes a notched specimen to fail at the same level of fracture toughness as pre-cracked test-pieces of the same material. From what has been said before,  $\rho_{eff}$  coincides with  $\underline{s}$ . Thus, experiments on notched specimens with  $0 < \rho < \underline{s}$  allow to determine the level of  $J_{IC}$  of the material, whereas tests on samples with  $\rho > \underline{s}$  are able to provide the inclination of the above referred sloped line from which  $\epsilon_{max,f}^*$  can be eventually derived (7).

Experimental verification of Eq. 1 was performed by testing three different 0.17% C - 1.33% Mn ferritic-pearlitic steels with increasing inclusion contents and  $\underline{s}$  of the order of 0.1 mm for all of them (4)(8): it yielded  $\rho_{eff}$ 's of the same order of magni-

tude as  $\underline{s}$ . It has been further proved (7) that the largest the inclusion volume fraction, the lowest the corresponding value of  $\epsilon_{\max, f}^*$  and therefore of  $J_{IC}$ .

Having demonstrated the feasibility of the application of Eq. 1 to adequately interpret fracture toughness data of mild steels, it can be concluded that, to increase the ductile fracture toughness of a steel of this class, one has either to reduce the second-phase volume fraction or to increase the interparticle spacing or both. To prove the assumption it has been decided to perform experiments on a steel carefully selected to have a composition similar to the above referred ones, an inclusion volume fraction intermediate in respect of the interval delimited by the values pertaining to the previously tested steel, but a value of  $\underline{s}$  much larger than before. Furthermore, with Eq. 1 already verified, it has also been possible to greatly reduce the number of tests necessary to single out both the sloped line in the  $J$ - $\rho$  field and the level of  $J_{IC}$ .

#### MATERIAL AND EXPERIMENTAL PROCEDURE

Table 1 reports the chemical composition of the C-Mn ferritic-pearlitic steel used in the experiments, along with its microstructural characteristics and room temperature tensile properties.

Tensile and three point bending specimens were fabricated from blanks cut from a steel plate. They had the major dimension in the direction transverse in respect of the plate rolling one. Fatigue pre-cracks and round notches with two  $\rho$  nominal values (0.05 and 0.25 mm, respectively smaller and larger than  $\underline{s}$ ) were machined with the plane in the TL orientation. Cross-section specimen dimensions are reported in Table 2. It has to be noted that the specimen width has been limited by the maximum machining depth allowed by the V-blunt notch cutters at our disposal.

Second-phase distribution characteristics were determined by quantitative image analysis on metallographic surfaces in the crack plane.

#### RESULTS

Experimental J-R curves, obtained by the ASTM E813-83 multiple specimen procedure, are plotted in Fig. 1. For the pre-cracked specimens all the data points within the exclusion lines have been validated with the method recommended in the standard. For the validation of results pertaining to the 0.05 mm notch root radius samples, basing ourselves on previous experiences (8), it has been decided to consider acceptable all the data comprised in the  $\Delta a$  interval extending from 0 to the value indicated by the intersection of the J-R curve with the 1.5 mm offset exclusion

**TABLE 1 - Chemical Composition, mechanical Properties and micro-structural Characteristics of the Steel.**

C (%)	Mn (%)	Si (%)	P (%)	S (%)	Cu (%)	Ni (%)	Cr (%)	Mo (%)	Al (%)
0.155	1.36	0.23	0.010	0.012	0.21	0.14	0.10	0.01	0.02
$\sigma_y$ (MPa)		$\sigma_{uts}$	N		$e_f$ (%)	f (%)		$\bar{s}$ (mm)	
348		521	0.186		30.4	0.360		0.145	

**TABLE 2 - Cross-section Dimensions of the specimens (mm).**

$\rho$	B	w	$\rho$	B	w	$\rho$	B	w
0	10	20	0.05	29	23	0.25	29	25

line drawn in the figure. Instead, for the specimens with  $\rho = 0.25$  mm, only the points at a crack extension smaller than 1.5 mm have been considered in the J- $\Delta a$  least square approximation. In this last case, in fact, the exclusion lines are undoubtedly vertical (see following paragraph). Furthermore, the widths of the large notch specimens have resulted to be smaller than prescribed by the standard, if their high  $J_C$  value is substituted in the formulas in place of the fracture toughness.

For determining the applied J level at the onset of the real crack advance in blunt notch samples, no blunting line approximation is really necessary, as already stated before (8), although for very small values of  $\rho$  some degree of blunting cannot be a priori excluded. From the figure it appears that the  $J_{IC}$  level indicated by the usual ASTM procedure almost exactly corresponds to the J value obtained by extrapolation to  $\Delta a = 0$  of the J-R curve pertaining to the sample with nominal  $\rho = 0.05$  mm. Other considerations on the argument will be developed in the discussion. As expected, results yielded by the specimen with the largest  $\rho$  lie on a line extrapolating to a  $J_C$  level much higher than  $J_{IC}$ .

On the other hand the parallelism among all the experimental

J-R curves is remarkable. It is thus possible to conclude that the resulting tearing modulus ( $T = 200$  ca.) is not affected by the bluntness of the initial stress concentration. What entails that, even in this respect, pre-cracking is not essential to the obtainment of reliable fracture toughness data. It has to be noted that  $T$  for the actual steel is nearly identical to the one pertaining to the toughest steel in the previous series of experiments (steel 1, ref. 8).

Critical values of  $J$ , determined as described before, have been reported in Fig. 2 as a function of the notch root radius. The  $J$ - $\rho$  trend, as depicted by the dotted line, has been derived in accordance with what has been said in the presentation of Eq.1. Then,  $\rho_{\text{eff}}$  is at the intersection of the dotted and solid lines (the last one drawn at the  $J_{Ic}$  level).

The first consideration that can be formulated upon analyzing Fig. 2 is the coincidence between  $\rho_{\text{eff}}$  and  $\underline{s}$ , both being equal to 0.14 mm ca. Though the detailed micro-mechanism that controls such a phenomenon is still not completely clarified, it appears justified to hypothesize that the mode I opening of the crack surfaces during the blunting is limited by a pinning effect due to second phase particles lying above and below the crack-tip at an average interparticle distance equal to  $\underline{s}$ .

As regards the sloped portion of the  $J$ - $\rho$  plot, the inclination evidenced by the experimental results ( $\approx 2000 \text{ MN/m}^2$ ) is somewhat higher than that foreseeable by comparing the inclusion volume fraction of the present and previously tested steels. It has to be noted here that the slightly lower yield stress of the steel used in this investigation has surely induced a lower degree of stress triaxiality at the root of the notch of the 0.25 mm  $\rho$  blunt specimens now brought to fracture. The resulting  $J_c$  value is therefore somewhat higher than should have been obtained for a fully plane strain series of specimens.

What entails to conclude that for obtaining reliable results without using precracked specimens, one should be careful to employ specimen with adequate width.

#### DISCUSSION

First of all, it is to be stated that the above reported results, obtained upon testing samples fabricated with a C-Mn ferritic-pearlitic steel with an overall composition almost identical to the steels used in a previous series of experiments (4, 8), but with a much larger inclusion spacing, clearly emphasize the decidedly great influence of this microstructural characteristic upon the fracture toughness of steels of such a class.

In fact, results of fracture toughness tests on varying

notch root radius specimens have once again demonstrated the congruence between the radius of curvature reached by the crack-tip upon blunting and the mean distance between larger sulfides embedded in the matrix. What further confirms that is absolutely permissible to substitute  $\underline{s}$  upon  $\rho_{\text{eff}}$ ; thus, the procedure that has led the authors to write Eq. 1 (4) is correct.

Moreover, the results of the present investigation further validate Eq. 1 in respect to its capability of adequately foresee fracture toughness values from microstructural analysis data. In fact, the comparison between the steel here tested and steel 1 of refs. 4 and 8 (with a similar value of inclination of the sloped portion of the  $J$ - $\rho$  plot) shows that to a 32% increase of  $\underline{s}$  corresponds a variation of  $J_{IC}$  in the same sense and not very different in quantity (44% ca.).

Therefore, while routine testing a series of mild steels of the same class, it is possible to determine the  $J_{IC}$  value pertaining to each steel by performing experiments on 0.25 mm notch root radius specimens, drawing a  $J$ - $\rho$  straight line passing through the origin of the  $J$ - $\rho$  field, entering the diagram at an abscissa equal to  $\underline{s}$ , and reading the  $J_{IC}$  on the ordinate axis. It is thus possible to avoid the costly precracking procedure.

One final consideration can be drawn from the complex of our experimental results on C-Mn ferritic-pearlitic steels. The mechanism described in the introduction illustrating the sequence of phenomena of crack-tip blunting, void formation around inclusions, and inter-void ligament forming, stretching, and rupturing allows to identify the onset of the critical crack growth with the crack-tip reaching the second row of inclusions in its advancing path. Such a hypothesis corresponds to a procedure of singling out the  $J_{IC}$  value on the  $J$ - $R$  curve pertaining to a fatigue precracked specimen by drawing a vertical from the origin with an offset equal to 2 times the interparticle spacing. Our results reported in Fig. 1 indeed permit to verify that the vertical at the  $\Delta a = 0.28$  mm offset identifies, on the precracked specimen  $J$ - $R$  curve, a  $J$  value very similar to the  $J_{IC}$  one obtained by the application of the E813-83 ASTM Standard. Furthermore, a similar correspondance can be exacted by considering the  $J$ - $R$  curves and the  $\underline{s}$  values of the previously tested steels (8). Therefore, the proposed procedure for identifying the critical value of  $J$  applied at mild steel specimens fracture initiation can be upheld.

#### CONCLUSIONS

Crack-tip blunting is one of the parameters that define the level of toughness in elastic-plastic fracture; the larger the radius of curvature achieved by a fatigue crack-tip prior to fracture, the greater the amount of plastic deformation intervening in the

## FRACTURE CONTROL OF ENGINEERING STRUCTURES – ECF 6

process zone around the stress concentration, and, therefore, the larger the material fracture toughness.

In previous papers (1) (4) the authors had proposed a model describing how the inclusion content and distribution in mild steels play the most significant role in the processes intervening at the crack-tip under increasing applied stresses, i.e. blunting, void nucleation around large particles, further straining of the remaining ligaments between voids up to an overall crack advance.

Experiments performed now and before on three point bending specimens with varying notch root radii, fabricated with several different C-Mn ferritic-pearlitic steels have allowed to establish a definite link between the spacing among larger inclusions and the limiting radius that can be achieved by the crack-tip prior to fracture nucleation. Thus an increase of  $\underline{s}$ , while keeping other microstructural features constant, leads to a corresponding increase of  $J_{IC}$ .

Results have also allowed to further validate a procedure of  $J_{IC}$  determination in mild steels based on fracture toughness testing of non-precracked specimens and quantitative metallographic analysis of the material structure.

Finally, a new procedure to identify the J-integral applied at onset of fracture of precracked specimens, without resorting to dubious blunting line approximations, has been proposed.

### SYMBOLS USED

- a = crack length in the SENB specimens.
- B = thickness of the SENB specimens.
- $\epsilon_{max}^*$  = maximum strain acting at the root of a notch while loading a notched specimen.
- $\epsilon_{max,f}^*$  = maximum strain acting at the root of a notch at fracture initiation in a notched specimen.
- f = total inclusion volume fraction (%).
- $F(\Gamma(N)) = [(N + 1/2) \cdot (N + 3/2) \cdot \Gamma(N + 1/2)] / [\Gamma(1/2) \cdot \Gamma(N + 1)]$ .
- $\Gamma$  = mathematical function gamma.
- $J_c$  = J-integral applied at fracture initiation from a blunt notch.
- N = strain hardening exponent in the Ramberg-Osgwood con-

stitutive law:  $\sigma/\sigma_y = [\epsilon/\epsilon_y]^N$ .

$\rho$  = notch root radius (mm).

$\underline{s}$  = mean spacing between major inclusions ( $\mu\text{m}$ ).

$\sigma_{\text{flow}}$  =  $(\sigma_y + \sigma_{\text{uts}})/2$ .

T = tearing modulus:  $(dJ/da)(E/\sigma_{\text{flow}}^2)$ .

w = width of SENB specimens.

#### REFERENCES

- (1) Firrao, D. and Roberti, R., "Interrelation among Microstructure, Crack-tip Blunting, and Ductile Fracture Toughness in Mild Steels", Proceedings of the 6th International Conference on Fracture (ICF6) on "Advances in Fracture Research", Edited by S.R.Valluri et al., Pergamon Press, Oxford, U.K., 1984.
- (2) Smith, R.F. and Knott, J.F., "Crack Opening Displacement and Fibrous Fracture in Mild Steel", in "Practical Applications of Fracture Mechanics to Pressure Vessel Technology", I. Mech. Eng., London, 1971.
- (3) Chipperfield, G.C. and Knott, J.F., Microstructure and Toughness of Structural Steels, Metals Techn., Vol. 2, 1975, pp. 45-51.
- (4) Firrao, D. and Roberti, R., "A Model for Plane Strain Ductile Fracture Toughness", in "Strength of Metals and Alloys", Edited by R.C. Gifkins, Pergamon Press, Oxford, U.K., 1982.
- (5) Hahn, G.T. and Rosenfield, A.R., "Metallurgical Factors Affecting Fracture Toughness of High Strength Aluminum Alloys", Met. Trans. A, Vol. 6A, 1975, pp. 653-668.
- (6) Rice, J.R., "A Path Independent Integral and the Approximate Analysis of Stress Concentration by Notches and Cracks", J. Appl. Mech., Trans. ASME E, Vol. 35, 1968, pp. 379-386.
- (7) Firrao, D. and Roberti, R., "Sui parametri microstrutturali che controllano la tenacità alla frattura degli acciai", Metall. Ital., Vol. 75, 1983, pp. 645-651.
- (8) Roberti, R., Silva, G., Firrao, D., and De Benedetti, B., "Influence of Notch Root Radius on Ductile Rupture Fracture Toughness Evaluation with Charpy-V Type Specimens", Int. J. Fatigue, Vol. 3, 1981, pp. 133-141.



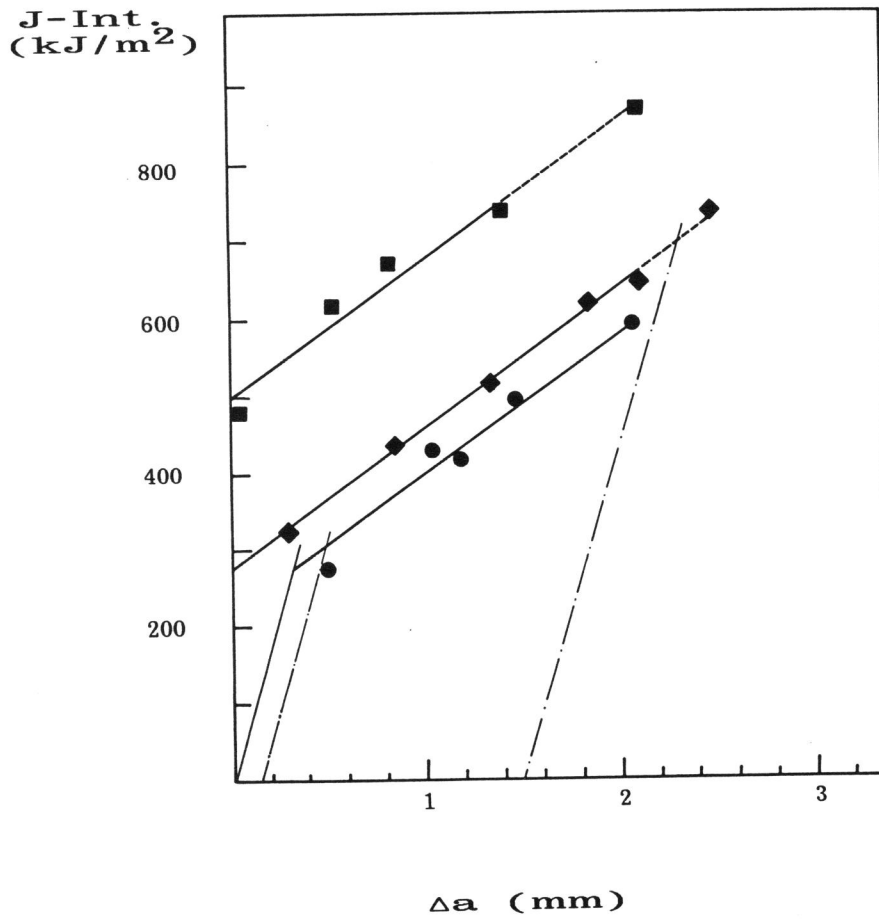


Figure 1 J resistance curves for sharp and blunt notches samples  
 (•:  $\rho \rightarrow 0$ ; ♦:  $\rho = 0.05$  mm; ■:  $\rho = 0.25$  mm)

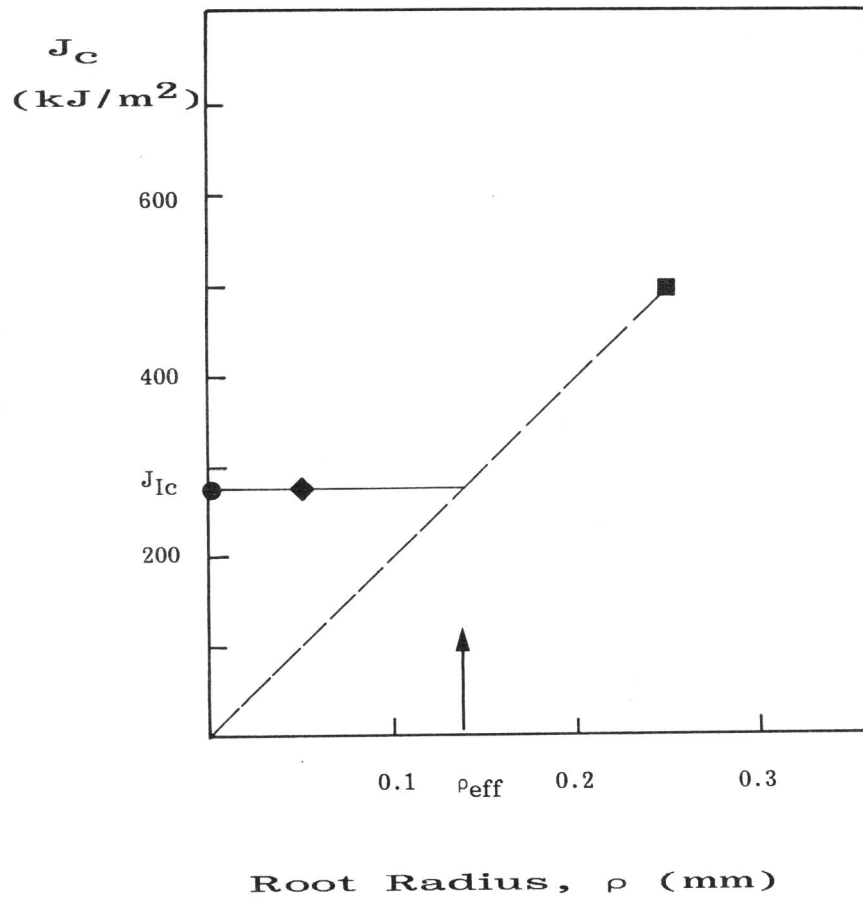


Fig 2 Variation of J-integral values applied at onset of fracture in sharp and blunt notch specimens